# Supermagnonic Propagation in Two-Dimensional Antiferromagnets

G. Fabiani, M. D. Bouman, and J. H. Mentink
*Radboud University, Institute for Molecules and Materials (IMM) Heyendaalseweg 135, 6525 AJ Nijmegen, Netherlands*

(Received 22 January 2021; revised 18 May 2021; accepted 15 July 2021; published 25 August 2021)

We investigate the propagation of magnons after ultrashort perturbations of the exchange interaction in the prototype two-dimensional Heisenberg antiferromagnet. Using the recently proposed neural quantum states, we predict highly anisotropic spreading in space constrained by the symmetry of the perturbation. Interestingly, the propagation speed at the shortest length scale and timescale is up to 40% higher than the highest magnon velocity. We argue that the enhancement stems from extraordinary strong magnon-magnon interactions, suggesting new avenues for manipulating information transfer on ultrashort length scales and timescales.

DOI: 10.1103/PhysRevLett.127.097202

*Introduction.*—The study of magnons, the collective spin excitations in magnetic systems, has triggered significant interest in recent years. Stimulated by the potential for high-speed low-energy data processing, high-energy coherent magnons are intensively investigated in the field of magnonics [1] and spintronics [2,3]. In addition, high-energy magnons have a crucial role in the microscopic dynamics of ultrafast switching between magnetically ordered states [4–8], and are potentially essential for the stabilization of various complex quantum many-body states [9–11]. Furthermore, these studies are greatly stimulated by the availability of femtosecond x-ray techniques [12], which ultimately can measure the propagation of magnons with nanometer spatial and femtosecond temporal resolution. Nevertheless, rather little is known about the propagation of high-energy magnons at these ultrashort length scales and timescales.

A direct way to access high-energy magnons is via optical perturbations of the exchange interactions [13], as well established in Raman spectroscopy, both in the frequency [14,15] and time domain [16–18]. In this approach, high-energy magnons are excited in pairs with wavelengths as small as the distance between two atoms, corresponding to oscillation frequencies determined by the exchange energy. Interestingly, the spectrum of these magnon pairs is significantly affected by magnon-magnon interactions [19–21]. This is particularly true for the case with strongest quantum spin fluctuations, i.e., the relevant case of spin $S = 1/2$ in two dimensions (2D) [20,22], for which even the single-magnon spectra are strongly modified at short wavelengths [23–31]. Hence, magnon-magnon interactions might have a pronounced effect on the propagation of high-energy magnons, especially in the systems for which experimentally the strongest quantum fluctuations are found [32,33]. Therefore, we aim to understand both *how* magnon-magnon interactions influence the propagation of magnon pairs, and to quantify *how strong* this effect becomes in the regime of strongest quantum fluctuations.

Theoretical investigation of magnon propagation in this deep quantum regime is highly challenging, since it requires to solve the unitary dynamics of an extended quantum many-body system with strong spatial and temporal quantum spin correlations, for which no exact methods exist. Recently, however, a new family of algorithms was proposed which are inspired by machine learning [34]. Although being inherently a variational method, these neural quantum states (NQSs) offer a nearly unbiased approach to the full quantum dynamics. In particular, it was shown that NQSs are highly efficient for the simulation of quantum spin dynamics in the most challenging 2D limit [35,36].

Here, we apply the NQS to investigate the propagation of magnons after ultrashort perturbations of the exchange interaction in the square lattice spin-1/2 antiferromagnetic Heisenberg model. We find that the correlation spreading resembles the anisotropic propagation pattern expected from noninteracting magnons. Interestingly, however, at the shortest length scales and timescales, we predict that the spreading speed qualitatively deviates from noninteracting magnons, reaching speeds that are significantly higher than the highest magnon group or phase velocity. By comparison with approximate results obtained with Schwinger boson mean-field theory (SBMFT), we identify that this enhanced spreading speed stems from an interplay between a localized quasibound state emerging from magnon-magnon interactions and propagating, nearly noninteracting magnon pairs. We predict 40% enhancement of the propagation speed in the regime of strongest quantum fluctuations.

*Model and method.*—We study the spin-1/2 antiferromagnetic Heisenberg model on a square lattice with $N = L \times L$ spins $\hat{\mathbf{S}}_i = \hat{\mathbf{S}}(\mathbf{r}_i)$, with $\mathbf{r}_i = (x_i, y_i)$

$$\hat{\mathcal{H}} = J_{\mathrm{ex}} \sum_{\langle ij \rangle} \hat{\mathbf{S}}_i \cdot \hat{\mathbf{S}}_j, \tag{1}$$

 © 2021 American Physical Society

where $J_{\mathrm{ex}}$ is the exchange interaction ($J_{\mathrm{ex}} > 0$) and $\langle\cdot\rangle$ restricts the sum to nearest neighbors. We consider the dynamics induced by a time-dependent perturbation of the exchange interaction [13,16–18,37,38], modeled by the perturbation

$$\delta\hat{\mathcal{H}}(t) = \Delta J_{\mathrm{ex}}(t)\frac{1}{2}\sum_{i,\boldsymbol{\delta}}(\mathbf{e}\cdot\boldsymbol{\delta})^2\hat{\mathbf{S}}(\mathbf{r}_i)\cdot\hat{\mathbf{S}}(\mathbf{r}_i+\boldsymbol{\delta}), \quad (2)$$

where $\mathbf{e}$ is a unit vector that determines the polarization of the electric field of the light pulse which causes the perturbation and $\boldsymbol{\delta}$ connects nearest neighbor spins. This perturbation is reminiscent to the Loudon-Fleury theory of spontaneous Raman scattering [39]. In the remainder of this work we set $\hbar = 1$ and the lattice constant $a = 1$, and work at zero temperature.

To simulate the real-time dynamics following Eq. (2) we employ the recently introduced neural quantum state ansatz inspired by machine learning [34]. This approximates the wave function of the system with a restricted Boltzmann machine (RBM) which can be expressed as

$$\psi = \exp\left(\sum_i a_i S_i^z\right)\prod_{i=1}^{M} 2\cosh\left(b_i + \sum_j W_{ij}S_j^z\right). \quad (3)$$

Here $S_i^z = \pm 1/2$ correspond to the physical spins and $\{a_i, b_i, W_{ij}\}$ are complex coefficients that parametrize the many-body wave function. The number of variational parameters is $N_{\mathrm{var}} = \alpha\times N^2 + \alpha\times N + N$, with $\alpha = M/N$ controlling the accuracy of the ansatz. The neural network is trained by means of variational Monte Carlo techniques to simulate the ground state and time-dependent states of a given lattice Hamiltonian. In particular, unitary dynamics is addressed by employing the time-dependent variational principle [40].

In a previous work we showed that the RBM ansatz can reproduce the ground-state properties of Eq. (1) and the dynamic properties under Eq. (2) with high accuracy [35]. Here we adopt a similar protocol approximating the time-dependent change of the exchange interaction as a global quench of $J_{\mathrm{ex}}$ along $\mathbf{e} = \mathbf{y}$ with $\Delta J_{\mathrm{ex}}(t) = 0.1 J_{\mathrm{ex}}\Theta(t)$, where $\Theta(t)$ is the Heaviside function. For the short-time dynamics considered here, this closely resembles the square pulse protocol adopted in [35]. Our numerical simulations always start from the ground state of Eq. (1) and are obtained using the ULTRAFAST code [35].

*Results.*—According to a well-established quasiparticle picture [41], the space-time dynamics of quantum correlations after a quench is determined by the quasiparticles excited. Therefore, to investigate the propagation of magnons triggered by Eq. (2), we consider the time evolution of

$$C(\mathbf{R},t) = \langle\hat{\mathbf{S}}_i(t)\cdot\hat{\mathbf{S}}_j(t)\rangle_{\mathrm{c}} - \langle\hat{\mathbf{S}}_i(0)\cdot\hat{\mathbf{S}}_j(0)\rangle_{\mathrm{c}}, \quad (4)$$

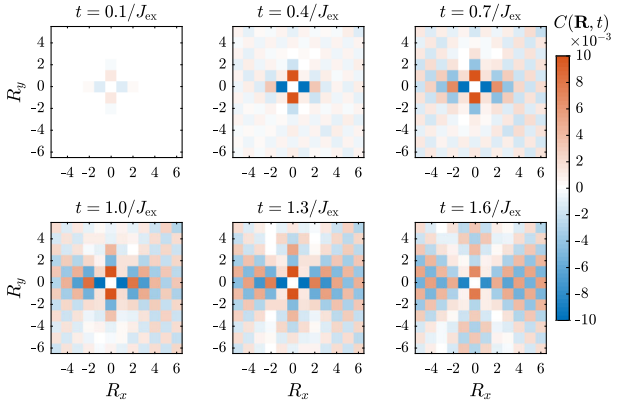


FIG. 1. (Color online) Snapshots in time of the postquench dynamics of spin correlations in an $L\times L = 12\times 12$ system simulated with the RBM ansatz ($\alpha = 16$). The figures reveal a clear spreading of correlations, with a nontrivial wavefront developing at ultrashort timescales. The checkerboard pattern reflects the antiferromagnetic coupling between spins. The noise in the correlations is due to Monte Carlo errors, and to improve readability the colormap is clipped at $\pm 10^{-2}$.

where $\langle\hat{A}\,\hat{B}\rangle_{\mathrm{c}} = \langle\hat{A}\,\hat{B}\rangle - \langle\hat{A}\rangle\langle\hat{B}\rangle$ and $\mathbf{R} = \mathbf{r}_i - \mathbf{r}_j$. Both the system and the perturbation are translationally invariant and therefore the correlation function only depends on the relative distance $\mathbf{R}$ between the sites considered. Figure 1 shows different snapshots in time of the correlator $C(\mathbf{R},t)$ obtained with the RBM ansatz in a $12\times 12$ lattice. We note that after $t\approx 1.6/J_{\mathrm{ex}}$ the wave front reaches the lattice boundaries and the subsequent spreading, dominated by finite-size effects, is not considered. Figure 1 reveals a propagation pattern arising at very small timescales with a highly anisotropic wave front, with almost vanishing correlations along the diagonals. The weak spreading along the diagonals derives from an exact symmetry of $C(\mathbf{R},t)$ that holds in the linear response limit $\Delta J_{\mathrm{ex}} \ll J_{\mathrm{ex}}$ (see Supplemental Material I [42]; a similar result was recently found in [43]). In this limit, the correlation function $C(\mathbf{R},t)$ is antisymmetric with respect to reflections over one of the diagonals of the lattice. As a consequence, $C(\mathbf{R},t)$ vanishes when $R_x = \pm R_y$. Small corrections beyond linear response break this symmetry, yielding a slight anisotropy between $\mathbf{x}$ and $\mathbf{y}$ axes, with finite (but small) correlations along the diagonals consistent with the spreading patterns of Fig. 1.

In order to extract the speed of the correlation spreading, we focus on the correlations along the $\mathbf{x}$ direction with $\mathbf{R} = (R_x, 0)$. Figure 2 shows the time evolution of such correlations in an $L\times L = 20\times 20$ system for $|R_x| \le 8$, with $\alpha = 12$. For this $\alpha$, convergence with the number of variational parameters is achieved. Moreover, we expect that correlations at least up to $|R_x| = 7$ are free from finite-size effects for the time interval considered here (see Supplemental Material IV). Note also that due to periodic boundary conditions and translation invariance $C(\mathbf{R},t) = C(L\hat{\mathbf{x}} - \mathbf{R}, t)$ up to Monte Carlo errors. Figure 2 shows

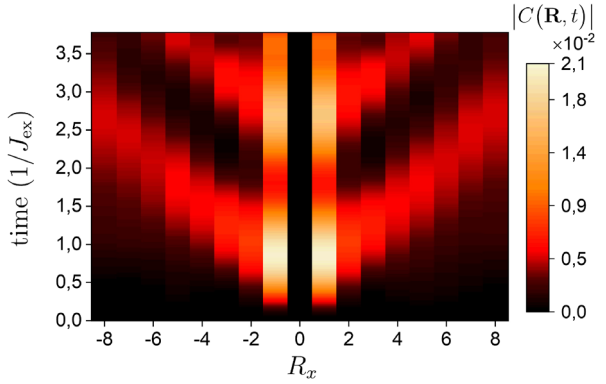


FIG. 2. (Color online) Time evolution of spin correlations $|C(\mathbf{R},t)|$ as a function of the distance $R_x$ in an $L\times L=20\times 20$ system. A light-cone-like spreading of correlations appears in agreement with the locality of $\hat{\mathcal{H}}+\delta\hat{\mathcal{H}}$. Results are obtained with the RBM ansatz using $\alpha=12$.

that, when considering correlations along one direction, a light-cone-like spreading of correlations emerges analogous to what is observed in one-dimensional systems [41,44–47]. An estimate of the light-cone slope, which gives the spreading speed of correlations, is obtained by fitting the time $t^*$ at which the first extrema appear as a function of $R_x$. In particular, we extract the speed from the inverse of the slope of the fitted line, which characterizes the velocity of correlation propagation between subsequent positions $R_x$. Figure 3(a) shows the arrival times $t^*$ averaged over positive and negative $R_x$ (red diamonds). The extracted velocity reveals a peculiar bending when going from small to larger distances ($|R_x|>5$), and a

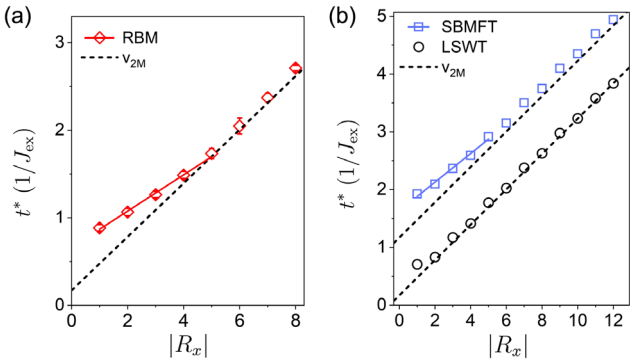


FIG. 3. (Color online) Arrival times $t^*$ of the first extrema of $C(\mathbf{R},t)$. (a) RBM data (red diamonds) compared with the highest magnon group velocity $v_{2M}$ (black dashed line). (b) Comparison between SBMFT (blue squares) and LSWT (black circles). Solid red (blue) line: fit of the $|R_x|\leq 5$ arrival times of the RBM (SBMFT) correlations. To improve readability, the SBMFT data have been shifted in time by $+1/J_{ex}$. The RBM points are calculated for $L\times L=20\times 20$ ($\alpha=12$), while the LSWT and SBMFT data refer to an $L\times L=140\times 140$ system, where finite-size convergence is found.

spreading speed of the first $|R_x|\leq 5$ correlations of $v(\mathrm{RBM})=(4.71\pm 0.13)J_{ex}$ (red solid line).

To interpret the results obtained we first turn to linear spin wave theory (LSWT), which is expected to give an accurate account of the correlation spreading for small perturbations and long wavelengths. To this end, the Hamiltonian and perturbation Eqs. (1) and (2) are expressed in terms of Holstein-Primakoff boson operators. Next, a Bogolyubov transformation is applied in momentum space such that the resulting linear terms of $\hat{\mathcal{H}}$ are diagonalized. Up to constant terms this yields ($t>0$)

$$\hat{\mathcal{H}}+\delta\hat{\mathcal{H}}(t)=\frac{1}{2}\sum_{\mathbf{k}}[(\omega_{\mathbf{k}}+\delta\omega_{\mathbf{k}})(\hat{\alpha}^{\dagger}_{\mathbf{k}}\hat{\alpha}_{\mathbf{k}}+\hat{\alpha}_{-\mathbf{k}}\hat{\alpha}^{\dagger}_{-\mathbf{k}}) + V_{\mathbf{k}}(\hat{\alpha}^{\dagger}_{\mathbf{k}}\hat{\alpha}^{\dagger}_{-\mathbf{k}}+\hat{\alpha}_{\mathbf{k}}\hat{\alpha}_{-\mathbf{k}})]. \quad (5)$$

Here $\omega_{\mathbf{k}}$ is the single-magnon dispersion renormalized by the Oguchi factor $Z_c$ [48], while $\delta\omega_{\mathbf{k}}$ and $V_{\mathbf{k}}$ are proportional to $\Delta J_{ex}$ and depend on the details of the perturbation. The first term describes the bare magnon spectrum, which is renormalized due to the perturbation of $J_{ex}$. The second term is responsible for the creation and annihilation of pairs of counterpropagating magnons. In this approximation, the dynamics of spin correlations can be solved analytically, yielding

$$C(\mathbf{R},t)=C_0(\mathbf{R})-\frac{1}{N}\sum_{\mathbf{k}}\Gamma_{\mathbf{k}}(e^{i\mathbf{k}\cdot\mathbf{R}+i2\omega_{\mathbf{k}}t}+e^{i\mathbf{k}\cdot\mathbf{R}-i2\omega_{\mathbf{k}}t}), \quad (6)$$

in the linear response limit $\Delta J_{ex}\ll J_{ex}$, where $C_0(\mathbf{R})$ is a time-independent term, $\Gamma_{\mathbf{k}}$ is a time-independent factor depending on the geometry of the system and on the perturbation. A detailed derivation is given in Supplemental Material II.

The spreading speed of the extrema of Eq. (6) is extracted with the same procedure exploited for the RBM correlations. Figure 3(b) shows the arrival times of the first extrema of Eq. (6) versus the distance $|R_x|$ (black circles). This is compared with the light-cone slope $v_{2M}$ determined by twice the highest group velocity [41], which in the linear response limit is $v_{2M}=2[(d\omega_{\mathbf{k}})/(d\mathbf{k})]|_{\mathbf{k}=0}\approx 3.28J_{ex}$ (dashed black line). We note that the latter also equals twice the highest phase velocity $[(2\omega_{\mathbf{k}})/(k_x)]|_{\mathbf{k}=0}$, which instead determines the spreading speed of the first extrema [47]. The LSWT results demonstrate that the RBM ansatz yields higher spreading speeds at small times and distances, $v(\mathrm{RBM})$ being more than 40% higher than the corresponding LSWT speed. Interestingly, the RBM spreading speed at $|R_x|>5$ decreases down to the expected two-magnon velocity as it appears in Fig. 3(a). We refer to the initial regime as *supermagnonic*, since the spreading speed of the correlations is much higher than obtainable from the single-magnon dispersion.

To qualitatively assess the effect of magnon-magnon interactions beyond the Oguchi correction, we consider a

SBMFT approximation of the 2D Heisenberg Hamiltonian [49,50]. This provides an exact solution of the SU($n$) generalization of the Heisenberg Hamiltonian in the limit $n \to \infty$, in which magnon-magnon interactions remain finite. In addition, opposed to LSWT, SBMFT does not assume a symmetry broken ground state.

Results for the correlation spreading within SBMFT are shown in Fig. 3(b) (blue squares), where the linear response dynamics is considered within the Zubarev formalism [51–53]. These results reveal an enhancement of the spreading speed of the first $|R_x| \leq 5$ correlations similar to what is obtained with the RBM ansatz and a speed $v(\mathrm{SBMFT}) = (4.06 \pm 0.24) J_{\mathrm{ex}}$ (blue solid line). Our calculations show that the SBMFT exhibits two features. Besides propagating modes closely resembling noninteracting two-magnon pairs, an additional quasibound state of two spin-flip excitations appears (see Supplemental Material III), similar to what is obtained with other interacting magnon theories [19–21]. The latter dominates the spectrum at small wavelengths, decreasing the frequency of the two-magnon peak as compared to twice the frequency of zone-edge magnons. These two spin-flip excitations are well known from Raman spectroscopy, since the short-range correlations dominate the Raman spectrum. The supermagnonic propagation, however, is a nontrivial effect arising from the interplay between the quasibound state and the propagating magnon pairs. At short distances, the decrease in frequency delays the arrival time of the maxima in Fig. 3(b). This delay rapidly reduces with distance, causing a crossover regime at enhanced speed, recovering the noninteracting propagation speed at large distances. In a semiclassical picture, this supermagnonic regime can therefore be understood as subballistic propagation of quasiparticles, which only interact when being in close vicinity to each other. As they propagate, the interaction strength decreases and the quasiparticles enter a ballistic regime consistent with the noninteracting two-magnon light cone. We emphasize that SBMFT also encompasses the Oguchi correction that renormalizes the single-magnon spectrum due to magnon-magnon interactions in LSWT. Hence, the appearance of the quasibound state results from magnon-magnon interactions between magnon pairs, and goes beyond the Oguchi correction of the single-magnon spectrum.

Within SBMFT, we can further tune the strength of magnon-magnon interactions by varying the spin value $S$. We find that as $S$ increases towards the classical limit $S \to \infty$, the result converges to that of LSWT (see Supplemental Material III). This shows that the significance of the supermagnonic spreading scales with the importance of quantum fluctuations. Overall, the SBMFT results suggest that the RBM data feature extraordinary strong magnon-magnon interactions, beyond what can be expected from standard interacting magnon-theories. This analysis is also consistent with the fact that standard interacting magnon theory fails to fully reproduce the exact frequency and width of the spontaneous Raman spectrum of $S = 1/2$ antiferromagnets in 2D [20,22,35,54].

To conclude this section, we comment on the possible experimental verification of the supermagnonic correlation spreading. An interesting material class is the spin-1/2 antiferromagnets comprising copper ions, such as $La_2CuO_4$ [23,25,55] and $Cu(DCOO)_2 \cdot 4D_2O$ (CFTD) [24,30]. For example, in CFTD the dominant nearest neighbor exchange is $J_{\mathrm{ex}} = 6.19$ meV. Hence, the fastest two-magnon oscillation period is $T = h/E_{\mathrm{max}} \approx 160$ fs, where the upper bound for $E_{\mathrm{max}} = 2Z_c \hbar\omega_{\mathrm{max}}(z-1)/z$ ($z$ being the lattice coordination number) is estimated from interacting magnon theory [20], using the single-magnon energy $\hbar\omega_{\mathrm{max}} \approx 15$ meV [24]. With a nearest-neighbor distance $a = 5.74$ Å, the supermagnonic velocity is $v \approx 4aJ_{\mathrm{ex}}/\hbar \sim 20$ km/s, and therefore the required experimental resolution is in the nanometer length scale and femtosecond timescale. This is in reach with femtosecond x-ray diffraction techniques, in particular when combined with transient gratings [56–59]. Moreover, the enhanced spreading speed is also present in systems with higher spin, for example, $S = 1$ which enriches the class of materials to fluorides [16–18].

*Conclusion.*—In this work we predicted that magnons in two dimensions can propagate with a velocity that is up to 40% higher than the highest magnon velocity. This supermagnonic speed stems from extraordinary strong magnon-magnon interactions and might be corroborated by femtosecond x-ray free electron laser experiments with nanometer resolution. Future works might also focus on studying the spreading pattern in detail, both by considering different excitation geometries in the square lattice and by investigating different lattices, such as honeycomb systems. The latter feature even larger quantum fluctuations due to the lower coordination number $z$ [60,61] and hence may therefore exhibit an enhanced supermagnonic regime. Furthermore, it will be interesting to gain insight into the role of fractionalized spin excitations [30,31] and magnon-Higgs scattering [28,29] on the space-time propagation of magnon pairs. Moreover, such propagation is generally accompanied by a linear growth of entanglement [41]. How this is affected by magnon-magnon interactions is currently under investigation.

This work is part of the Shell-NWO/FOM-initiative "Computational sciences for energy research" of Shell and Chemical Sciences, Earth and Life Sciences, Physical Sciences, FOM and STW, and received funding from the European Research Council ERC grant agreement No. 856538 (3D-MAGiC). Part of this work was carried out on the Dutch national e-infrastructure with the support of SURF Cooperative.

*Note added in the proof.*—After completion of our manuscript we became aware of the following work [43], in

which the same spatial asymmetry in the spin correlations was found as we show in Fig. 1. Due to the smaller system size, the supermagnonic effect could not be resolved in that study.


[1] A. V. Chumak, V. Vasyuchka, A. Serga, and B. Hillebrands, Nat. Phys. **11**, 453 (2015).
[2] , D. Grundler, Nat. Nanotechnol. **11**, 407 (2016).
[3] J. Wang, Y. K. Takahashi, and Ki Uchida, Nat. Commun. **11**, 2 (2020).
[4] I. Radu, K. Vahaplar, C. Stamm, T. Kachel, N. Pontius, H. A. Dürr, T. A. Ostler, J. Barker, R. F. L. Evans, R. W. Chantrell *et al.*, Nature (London) **472**, 205 (2011).
[5] C. E. Graves, A. H. Reid, T. Wang, B. Wu, S. de Jong, K. Vahaplar, I. Radu, D. P. Bernstein, M. Messerschmidt, L. Müller *et al.*, Nat. Mater. **12**, 293 (2013).
[6] E. Iacocca, T.-M. Liu, A. H. Reid, Z. Fu, S. Ruta, P. W. Granitzka, E. Jal, S. Bonetti, A. X. Gray, C. E. Graves *et al.*, Nat. Commun. **10**, 1756 (2019).
[7] S. Ruta, Z. Fu, T. Ostler, A. Kimel, and R. Chantrell, arXiv:2006.07935.
[8] F. Büttner, B. Pfau, M. Böttcher, M. Schneider, G. Mercurio, C. M. Günther, P. Hessing, C. Klose, A. Wittmann, K. Gerlinger *et al.*, Nat. Mater. **20**, 30 (2021).
[9] F. Novelli, G. De Filippis, V. Cataudella, M. Esposito, I. Vergara, F. Cilento, E. Sindici, A. Amaricci, C. Giannetti, D. Prabhakaran *et al.*, Nat. Commun. **5**, 5112 (2014).
[10] M. P. M. Dean, Yue Cao, X. Liu, S. Wall, D. Zhu, R. Mankowsky, V. Thampy, X. M. Chen, J. G. Vale, D. Casa *et al.*, Nat. Mater. **15**, 601 (2016).
[11] D. G. Mazzone, D. Meyers, Y. Cao, J. G. Vale, C. D. Dashwood, Y. Shi, A. J. A. James, N. J. Robinson, J. Q. Lin, V. Thampy *et al.*, Proc. Natl. Acad. Sci. U.S.A. **118**, e2103696118 (2021).
[12] M. Buzzi, M. Först, R. Mankowsky, and A. Cavalleri, Nat. Rev. Mater. **3**, 299 (2018).
[13] J. H. Mentink, J. Phys. Condens. Matter **29**, 453001 (2017).
[14] W. H. Weber and R. Merlin, *Raman Scattering in Materials Science* (Springer Berlin Heidelberg, Berlin, Heidelberg, 2000).
[15] T. P. Devereaux and R. Hackl, Rev. Mod. Phys. **79**, 175 (2007).
[16] J. Zhao, A. V. Bragas, D. J. Lockwood, and R. Merlin, Phys. Rev. Lett. **93**, 107203 (2004).
[17] D. Bossini, S. Dal Conte, Y. Hashimoto, A. Secchi, R. V. Pisarev, Th. Rasing, G. Cerullo, and A. V. Kimel, Nat. Commun. **7**, 10645 (2016).
[18] D. Bossini, S. Dal Conte, G. Cerullo, O. Gomonay, R. V. Pisarev, M. Borovsak, D. Mihailovic, J. Sinova, J. H. Mentink, Th. Rasing, and A. V. Kimel, Phys. Rev. B **100**, 024428 (2019).
[19] R. J. Elliott and M. F. Thorpe, J. Phys. C **2**, 1630 (1969).
[20] C. M. Canali and S. M. Girvin, Phys. Rev. B **45**, 7127 (1992).
[21] J. Lorenzana and G. A. Sawatzky, Phys. Rev. B **52**, 9576 (1995).
[22] A. W. Sandvik, S. Capponi, D. Poilblanc, and E. Dagotto, Phys. Rev. B **57**, 8478 (1998).
[23] R. Coldea, S. M. Hayden, G. Aeppli, T. G. Perring, C. D. Frost, T. E. Mason, S.-W. Cheong, and Z. Fisk, Phys. Rev. Lett. **86**, 5377 (2001).
[24] N. B. Christensen, H. M. Rønnow, D. F. McMorrow, A. Harrison, T. G. Perring, M. Enderle, R. Coldea, L. P. Regnault, and G. Aeppli, Proc. Natl. Acad. Sci. U.S.A. **104**, 15264 (2007).
[25] N. S. Headings, S. M. Hayden, R. Coldea, and T. G. Perring, Phys. Rev. Lett. **105**, 247001 (2010).
[26] M. P. M. Dean, R. S. Springell, C. Monney, K. J. Zhou, J. Pereiro, I. Božović, B. Dalla Piazza, H. M. Rønnow, E. Morenzoni, J. van den Brink, T. Schmitt, and J. P. Hill, Nat. Mater. **11**, 850 (2012).
[27] M. Le Tacon, G. Ghiringhelli, J. Chaloupka, M. Moretti Sala, V. Hinkov, M. W. Haverkort, M. Minola, M. Bakr, K. J. Zhou, S. Blanco-Canosa *et al.*, Nat. Phys. **7**, 725 (2011).
[28] M. Powalski, G. S. Uhrig, and K. P. Schmidt, Phys. Rev. Lett. **115**, 207202 (2015).
[29] M. Powalski, K. P. Schmidt, and G. S. Uhrig, SciPost Phys. **4**, 001 (2018).
[30] B. Dalla Piazza, M. Mourigal, N. B. Christensen, G. J. Nilsen, P. Tregenna-Piggott, T. G. Perring, M. Enderle, D. F. McMorrow, D. A. Ivanov, and H. M. Rønnow, Nat. Phys. **11**, 62 (2015).
[31] H. Shao, Y. Q. Qin, S. Capponi, S. Chesi, Z. Y. Meng, and A. W. Sandvik, Phys. Rev. X **7**, 041072 (2017).
[32] K. B. Lyons, P. A. Fleury, J. P. Remeika, A. S. Cooper, and T. J. Negran, Phys. Rev. B **37**, 2353 (1988).
[33] R. R. P. Singh, P. A. Fleury, K. B. Lyons, and P. E. Sulewski, Phys. Rev. Lett. **62**, 2736 (1989).
[34] G. Carleo and M. Troyer, Science **355**, 602 (2017).
[35] G. Fabiani and J. H. Mentink, SciPost Phys. **7**, 004 (2019).
[36] M. Schmitt and M. Heyl, Phys. Rev. Lett. **125**, 100503 (2020).
[37] J. H. Mentink, K. Balzer, and M. Eckstein, Nat. Commun. **6**, 6708 (2015).
[38] R. V. Mikhaylovskiy, E. Hendry, A. Secchi, J. H. Mentink, M. Eckstein, A. Wu, R. V. Pisarev, V. V. Kruglyak, M. I. Katsnelson, Th. Rasing, and A. V. Kimel, Nat. Commun. **6**, 8190 (2015).
[39] P. A. Fleury and R. Loudon, Phys. Rev. **166**, 514 (1968).
[40] G. Carleo, F. Becca, M. Schiró, and M. Fabrizio, Sci. Rep. **2**, 243 (2012).
[41] P. Calabrese and J. Cardy, Phys. Rev. Lett. **96**, 136801 (2006).
[42] See Supplemental Material at http://link.aps.org/supplemental/10.1103/PhysRevLett.127.097202 for details about the derivation of the LSWT results, the derivation of the SBMFT results, the dependence on the spin $S$ of the supermagnonic effect within SBMFT and the convergence checks of the numerical results obtained with NQS.
[43] K. Tsutsui, K. Shinjo, and T. Tohyama, Phys. Rev. Lett. **126**, 127404 (2021).
[44] S. Bravyi, M. B. Hastings, and F. Verstraete, Phys. Rev. Lett. **97**, 050401 (2006).
[45] V. Alba and P. Calabrese, SciPost Phys. **4**, 017 (2018).

[46] K. R. A. Hazzard, M. van den Worm, M. Foss-Feig, S. R. Manmana, E. G. Dalla Torre, T. Pfau, M. Kastner, and A. M. Rey, Phys. Rev. A **90**, 063622 (2014).
[47] L. Cevolani, J. Despres, G. Carleo, L. Tagliacozzo, and L. Sanchez-Palencia, Phys. Rev. B **98**, 024302 (2018).
[48] T. Oguchi, Phys. Rev. **117**, 117 (1960).
[49] A. Auerbach and D. P. Arovas, Phys. Rev. Lett. **61**, 617 (1988).
[50] S. Sarker, C. Jayaprakash, H. R. Krishnamurthy, and M. Ma, Phys. Rev. B **40**, 5028 (1989).
[51] D. N. Zubarev, *Nonequilibrium Statistical Thermodynamics* (Consultants Bureau, New York, 1974).
[52] M. D. Bouman, Master's thesis, Radboud University, 2020.
[53] M. D. Bouman and J. H. Mentink (to be published).
[54] Y. R. Wang, M. J. Rice, and H. Y. Choi, Phys. Rev. B **44**, 9743 (1991).
[55] K. B. Lyons, P. A. Fleury, J. P. Remeika, A. S. Cooper, and T. J. Negran, Phys. Rev. B **37**, 2353(R) (1988).
[56] F. Bencivenga, R. Cucini, F. Capotondi, A. Battistoni, R. Mincigrucci, E. Giangrisostomi, A. Gessini, M. Manfredda, I. P. Nikolov, E. Pedersoli *et al.*, Nature (London) **520**, 205 (2015).
[57] M. Beye, R. Y. Engel, J. O. Schunck, S. Dziarzhytski, G. Brenner, and P. S. Miedema, J. Phys. Condens. Matter **31**, 014003 (2019).
[58] C. Svetina, R. Mankowsky, G. Knopp, F. Koch, G. Seniutinas, B. Rösner, A. Kubec, M. Lebugle, I. Mochi, M. Beck *et al.*, Opt. Lett. **44**, 574 (2019).
[59] D. Weder, C. von Korff Schmising, C. M. Günther, M. Schneider, D. Engel, P. Hessing, C. Strüber, M. Weigand, B. Vodungbo, E. Jal *et al.*, Struct. Dyn. **7**, 054501 (2020).
[60] S. S. Rosenblum and R. Merlin, Phys. Rev. B **59**, 6317 (1999).
[61] K. Kim, S. Y. Lim, JU. Lee, S. Lee, T. Y. Kim, K. Park, G. S. Jeon, CH. Park, JG. Park, and H. Cheong, Nat. Commun. **10**, 345 (2019).